

Article

Investigating the Result of Current Density, Temperature, and Electrolyte Concentration on COD: Subtraction of Petroleum Refinery Wastewater Using Response Surface Methodology

Sharon Chakawa and Mujahid Aziz * 

Environmental Engineering Research Group (EnvERG), Department of Chemical Engineering, Faculty of Engineering and the Built Environment, Cape Peninsula University of Technology, Bellville, P.O. Box 1906, Cape Town 7535, South Africa; btechresearch.aziz@gmail.com

* Correspondence: azizm@cput.ac.za; Tel.: +27-(0)21-460-4292

Abstract: Electrochemical oxidation (EO) investigated chemical oxygen demand (COD) subtraction from petroleum refinery wastewater (PRW) as a capable remediation process. Titanium substrates coated with iridium–tantalum oxide mixtures (Ti/IrO₂–Ta₂O₅) were used as the dimensional stable anode (DSA). The Box-Behnken Design (BBD), a statistical experimental design and response surface methodology (RSM), was used to matrix the current density, temperature, and electrolyte (NaCl) concentration variables, with COD removal efficiency as the response factor. A second-order verifiable relationship between the response and independent variables was derived where the analysis of variance displayed a high coefficient of determination value ($R^2 = 0.9799$). The predicted values calculated with the model equations were very close to the experimental values where the model was highly significant. Based on the BBD for current density, the optimum process conditions, temperature and electrolyte (NaCl) concentration were 7.5 mA/cm², 42 °C and 4.5 g/L, respectively. They were resulting in a COD removal efficiency of 99.83% after a 12-hour EO period.

Keywords: box-behnken design; electrochemical oxidation; petroleum refinery wastewater; chemical oxygen demand; response surface methodology; remediation; dimensional stable anode



Citation: Chakawa, S.; Aziz, M. Investigating the Result of Current Density, Temperature, and Electrolyte Concentration on COD: Subtraction of Petroleum Refinery Wastewater Using Response Surface Methodology. *Water* **2021**, *13*, 835. <https://doi.org/10.3390/w13060835>

Academic Editors: Giovanni Libralato and Alexandros I. Stefanakis

Received: 31 January 2021

Accepted: 16 March 2021

Published: 18 March 2021

Publisher's Note: MDPI stays neutral with regard to jurisdictional claims in published maps and institutional affiliations.



Copyright: © 2021 by the authors. Licensee MDPI, Basel, Switzerland. This article is an open access article distributed under the terms and conditions of the Creative Commons Attribution (CC BY) license (<https://creativecommons.org/licenses/by/4.0/>).

1. Introduction

Global demand for petroleum products is increasing rapidly; thus, our environment is exposed to rising hazardous impacts. One of these issues comes from large quantities of wastewater produced during crude oil processing, where approximately 0.6–1.4 of wastewater per ton of oil generated has high levels of contaminants [1]. It is estimated that the petroleum refinery industry generates an average of 5.34 billion litres per day of wastewater globally [2]. South Africa produces approximately 115 million litres of oil a day through six refineries by consuming 177 million litres of freshwater and generating about 137 million wastewater [3]. These high water demands and consumption have resulted in water becoming increasingly scarce and reducing groundwater levels, thus increasing water shortages in many areas [4]. Effluents from petroleum refinery are significant pollution sources that exhibit high concentrations of organic and inorganic pollutants and are characterised by high concentrations of chemical oxygen demand, fats, oil and grease, and phenol [2]. These pollutants have various adverse impacts on the surrounding environment. Due to the existence of these pollutants, petroleum refinery wastewater (PRW) is categorised as a hazardous waste by many environmental regulations worldwide [5]. Therefore, before discharging the wastewater into the environment, the amounts of these contaminants must be lowered to acceptable levels [6,7].

In recent years, advanced treatment methods, such as electrochemical [8], ozonation [9], and photocatalytic oxidation [10], have been described as effective for the treatment of petroleum refinery wastewater. Electrocoagulation (EC) and electrochemical oxidation

(EO) are more efficient than others in treating petroleum refinery wastewater (PRW). The EO process shows a unique advantage that electrical energy instead of chemical reagents is employed to degrade organic compounds. It is a clean process, a simple operation, and a small footprint of the treatment device [8]. Previous studies, such as by Park et al. (2012) [9] and Shestakova et al. (2014) [10], mainly focused on the study of electrodes with high oxygen growth potential for minimising the effect of bubbles. The mixed metal oxide (MMO) electrodes, Ti/IrO₂-Ta₂O₅, exhibited good electro-catalytic action and electrochemical stability due to their suitable IrO₂ loading [11]. A chemical reaction concerning the loss of one or more electrons on the anode surface by an atom or molecule formed from catalyst product during the passage through the anode, cathode, and electrolyte solution of the direct electrical current [12]. To break down even the most resistant organic compounds, EO is considered a very effective method. Organic pollutant anodic oxidation can occur in different ways, including direct and indirect oxidation [13].

The removal of chemical oxygen demand (COD) from electrochemical oxidation can be optimised by different variables that significantly affect the removal rate. The temperature [14], sodium chloride (NaCl) concentration [15], and current density [16] are some of the variables commonly studied concerning the removal of organic pollutants. The nature of other factors also determines the effect of one factor. According to Raju et al. (2008) [17], researchers have historically used multivariate systems to optimise the process by researching one factor at a time (OFAT). The OFAT approach was once considered the standardised, systematic, and acknowledged scientific experimentation method [18]. However, it has been proven that this method is inefficient and can potentially be catastrophic. This approach's main pitfalls are that more runs are needed for the same accuracy in effect estimation, do not predict interactions between the process's operational factors, and skip optimum factor settings [19].

To avoid this, a statistical multivariable experimental study approach, which is widely known as response surface methodology (RSM), was employed [20]. RSM is a helpful tool since it allows estimating several factor effects and their interactions on one or more response variables [21]. RSM includes a complete factorial design, central composite design, and Box-Behnken design (BDD) [22]. The BDD is a practical choice and an effective alternative to the full factorial and central composite design [23] due to its cost-efficiency and less time consumption [24]. Previous studies have shown the successful application of BDD in several processes, such as photoelectro-persulfate, ultrasound, adsorption, and electrochemical treatment [25–28].

Although previous studies have used RSM to investigate how different factors affect COD reduction of various types of wastewater, this research focused on PRW remediation and recycling in the South African Industrial context. Thus, this study aims to optimise the EO process to remove COD using the BDD at operational parameters NaCl concentration, temperature and current density.

2. Materials and Methods

2.1. Materials

High-grade chemicals and reagents were used for this research. Sodium chloride (NaCl), purchased from Merck, was used as the supporting electrolyte, and COD reagents were purchased from Hanna Instruments. All solutions used in this study were composed using water from an ultrapure Milli-Q purification system (MQ, Millipore).

2.2. Experimental Setup

A laboratory-scale EO system used in this study is shown in Figure 1. The system consisted of a glass reactor, water bath (FMH instrument), DC (Direct Current) power supply and two Ti/IrO₂-Ta₂O₅ electrodes (NMT electrodes, Pinetown, South Africa). The EO reactor had a total working volume of 1 L and was submerged in a water bath (FMH instruments) equipped with an immersion heating unit to keep the temperature constant. The two Ti/IrO₂-Ta₂O₅ electrodes used were immersed in the wastewater and served as

anode and cathode with a total effective area of 200 cm². The DC power supply was used to supply current to the EO system. All the EO experiments were conducted at an electrolysis time of 12 hours. The electrolysis time of 12 hours was determined to yield optimum removal efficiency based on the current experimental conditions [7]. The parameters used for the study were temperature (20 °C, 40 °C, and 60 °C), current density (5, 7.5, and 10 mA/cm²) and NaCl concentration as a supporting electrolyte (2, 4, and 6 g/L) [29]. The temperature steadily raised with an increase in electrolysis time. Therefore, the EO reactor was cooled with a cooling jacket. The initial pH was kept constant at an optimal 4 to ensure removal efficiency [8]. Samples were taken after 12 hours, and each run was duplicated.

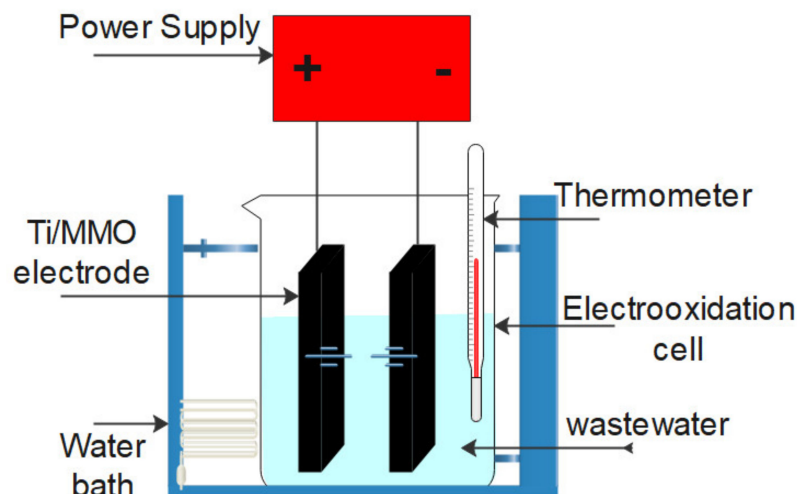


Figure 1. A schematic diagram for an electrochemical oxidation (EO) process.

2.3. Analytical Method

All equipment and meters were calibrated and checked according to the manufacturer's instruction. Electron Conductivity (EC) and temperature (T) were measured using a Crison CM 35+ handheld 147 meters (Merck Pty Ltd. South Africa). The pH calculated with Jenway 3510 Bench pH/mV Meter and Turbidity with an HF 148 Scientific Micro TPI. Infrared Turbidity Meter. COD samples were dissolved in a Thermo reactor Model 149 HI839800-02 (Hanna Pty Ltd., Cape Town, South Africa) and calculated using a COD Meter and Multiparameter photometer Model 150 HI83214-02 (Hanna Pty Ltd.).

2.4. Experimental Design

In the present study, the RSM analysis has been used to determine the relationship between the COD removal model and the optimum operating conditions. The BBD of RSM was chosen to determine the relationship between the response function and the variables using the Design-Expert (version 11.1.2.0, Stat ease Inc., Minneapolis, MN, USA). The range and level of independent variables were considered at three levels (Table 1).

Table 1. The levels and range of independent variables chosen for EO.

Symbols	Independent Variables	Units	Coded Levels		
			−1	0	+1
A	Temperature	°C	20	40	60
B	NaCl Concentration	g/L	2	4	6
C	Current Density	mA/cm ²	5	7.5	10

A second-order polynomial model given below was fitted to the experimental data for COD removal [30]

$$y = \beta_0 + \beta_1x_1 + \beta_2x_2 + \beta_3x_3 + \beta_{11}x_1^2 + \beta_{22}x_2^2 + \beta_{33}x_3^2 + \beta_{12}x_1x_2 + \beta_{13}x_1x_3 + \beta_{23}x_2x_3 \quad (1)$$

where y is the COD removal in coded units, β_0 is a constant, β_1 , β_2 , and β_3 are the regression coefficients for linear effects, β_{11} , β_{22} , and β_{33} are the quadratic coefficients, β_{12} , β_{13} , and β_{23} are the interaction coefficients and x_1 , x_2 , and x_3 are the operating variables. β is the correlation coefficient. With a 95% confidence level, P -value was used to evaluate the effect of model functions [31].

The Box-Behnken design (BBD) was used in this study. In this design, each factor was tested on three levels. BBD method is advantageous as it is sensitive to outliers, missing data, and default setting reduces the average prediction variances, resulting in a robust model with outstanding prediction characteristics [32]. The design matrix indicating experimental run order and output data for the BDD can be seen in Table 2.

Table 2. Box-Behnken Design output (responses) results.

Run	Independent Variables			COD Removal (%)	
	A: Temperature (°C)	B: NaCl Concentration (g/L)	C: Current Density (mA/cm ²)	Experimental Values	Predicted Values
1	40	2	7.5	87.00	87.28
2	40	4	7.5	91.70	90.89
3	40	6	7.5	90.20	89.92
4	60	2	10	84.90	84.95
5	20	4	7.5	88.20	88.50
6	20	6	10	86.20	86.73
7	40	4	10	90.60	90.87
8	20	2	10	85.90	85.52
9	40	4	5	89.10	89.43
10	20	2	5	83.70	83.90
11	20	6	5	86.00	85.75
12	60	6	10	89.10	88.38
13	40	6	10	89.70	89.74
14	60	2	5	83.40	83.05
15	60	4	7.5	88.50	88.90
16	60	6	5	86.70	87.12

The model investigated the influence of temperature (A), NaCl concentration (B), and current density (C) on the EO process using COD removal. The experimental results indicated that the COD removal was significantly affected by these parameters (independent variables). The results indicated that a maximum COD removal of 91.7% was achieved at temperature, NaCl concentration and current density of 40 °C, 4 g/L and 7.5 mA/cm², respectively. This experimental run was conducted over a 12-hour electrolysis period. The experimental results compare well with the optimised, predicted COD removal percentage. A close correlation between experimental and predicted values was found when a fair agreement was reached between the coefficient of determination (R^2) predicted.

3. Results and Discussion

3.1. Model Fitting

The data attained from 16 experimental runs were fitted into a second-order polynomial model equation to determine the relationship between the coded factors and the response, as shown in Equation (2).

The ANOVA analysis for the Box-Behnken design where A is temperature, B the NaCl concentration, and C the current density, is summarised in Table 3. The ANOVA was used to evaluate the determination coefficient, lack of fit, and the importance of the linear, squared, and interaction effects on the independent variables' response. The p -value was used to determine the significance of the coefficient and the combined factors' interaction

strength. Based on the F-test and P-test, the adequacy of the model in ANOVA research is acknowledged. The regression equation's response variation may be explained if the f -test value becomes higher than the p -value. The p -value is used to evaluate whether f is large enough to signal statistical significance [32].

$$\text{COD Removal \%} = 90.89 + 0.2A + 1.32B + 0.72C + 0.56AB + 0.068AC - 0.16BC - 2.19A^2 - 2.29B^2 - 0.74C^2 \quad (2)$$

Table 3. Analysis of variation (ANOVA) of the quadratic model.

Source	Sum of Squares	Df	Mean Square	F-Value	p -Value
Model	176.58	9	19.62	119.22	<0.0001 ¹
A-Temperature	0.80	1	0.80	4.86	0.0382 ¹
B-NaCl concentration	37.02	1	37.02	224.96	<0.0001 ¹
C-Current Density	11.02	1	11.02	66.98	<0.0001 ¹
AB	4.95	1	4.95	30.08	<0.0001 ¹
AC	0.076	1	0.076	0.46	0.5049 ²
BC	0.45	1	0.45	2.75	0.1117
A ²	29.58	1	29.58	179.74	<0.0001
B ²	28.09	1	28.09	170.66	<0.0001
C ²	2.92	1	2.92	17.76	0.0004
Residual	3.62	22	0.16		
Lack of Fit	2.69	6	0.45	7.66	0.0005 ¹
Pure Error	0.93	16	0.058		
Corr. Total	180.20	31			
Std. Deviation	0.41			R-Squared	0.9799
Mean	87.56			Adjusted R ²	0.9717
Coefficient of variation %	0.46			Predicted R ²	0.9564

Df-degree of freedom ¹ significant ² not significant.

The respective variables indicated a highly significant model when the p -value is smaller, and this was confirmed by Abbas et al. (2020) [33]. According to Table 3, the model's p -value is less than 0.0001, which indicated that the predicted quadratic model was significantly fitted. The independent variables, temperature (A), NaCl (B), current density and the interaction factor AB, showed the most significant effect on COD removal with $p < 0.05$. The interaction terms AC and BC were not significant. The p -value of the lack of fit was 0.0005, implying that the lack of fit was significant relative to the model's pure error.

Fit statistics are shown in Table 4. The coefficient of determination R² is a statistical parameter that measures how well the data fits the line [34]. A close correlation in experimental and predicted values were found when there was a reasonable agreement between predicted R² (0.9564) and adjusted R² (0.9717). The difference between the predicted and adjusted R² should be less than 0.2 for the model to be considered well fitted and able to make satisfactory predictions.

Table 4. Fit statistics.

	R ²	Adjusted R ²	Predicted R ²
COD reduction efficiency %	0.9799	0.9717	0.9564

For this study, predicted and adjusted R² agreed with this. The high value of the determination coefficient (R² = 0.9799) indicated enough mathematical model modification. This R² value showed that the model could describe variations of 97.99% in response to independent variables. A low coefficient of variation value of 0.46 indicated an accurate, reproducible and reliable model [35]. Hence, the regression model is significant.

3.2. Validation of Model

After the regression model was developed, the fitted model was tested to ensure an accurate approximation to the actual system was provided. Thangam et al. (2014) [36] stated

that optimising the fitted response surface is likely to produce inadequate or misleading performance if the model is not adequately fitted. Three types of model diagnostics were used for verification: the normal, residual, and predicted vs. experimental plot.

The evaluation of the predicted and experimental values of COD removal is presented in Figure 2. It can be observed that the data scattered closer to the 45-degree line, resulting in a higher determination coefficient above 0.9. This specifies that more than 90% of each independent variable in this study went through the modelling equation presented in Equation (1). Therefore, the agreement between the predicted and experimental COD removal values is adequate and per the statistical significance of the quadratic model produced.

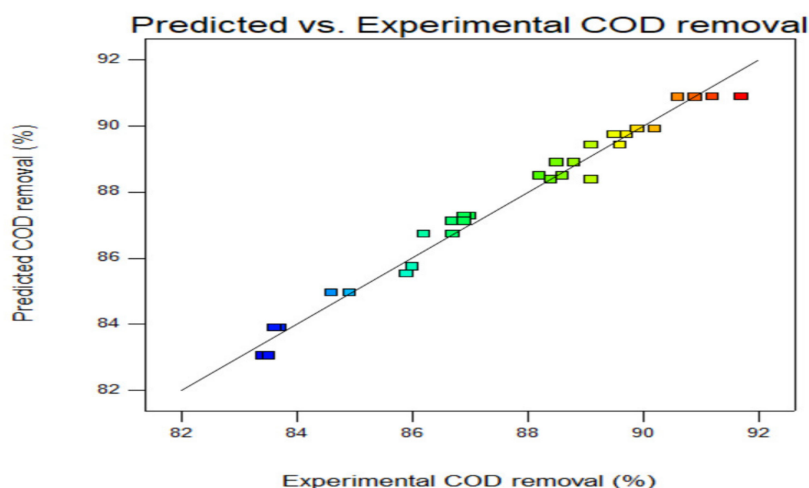


Figure 2. Predicted vs. experimental COD removal values.

The normality probability plot of the residual was constructed to investigate the independability of linear regression. The graph in Figure 2 displays the scatter of residuals in a linear format. Several points lie very close to and on the regression line, indicating a perfect fit of the model compared to the data. The upper and lower normal percentage probabilities are also located close to the line. This shows that the model has a perfect fit at the boundary points, as well. Thus, the normality percentage probability plot (Figure 3) showed that the exact values provided enough estimation to the model. These findings are like the ones obtained by Darvishmotevalli et al. (2019) [37]. Furthermore, this confirms the accuracy of the Box-Behnken experimental design.

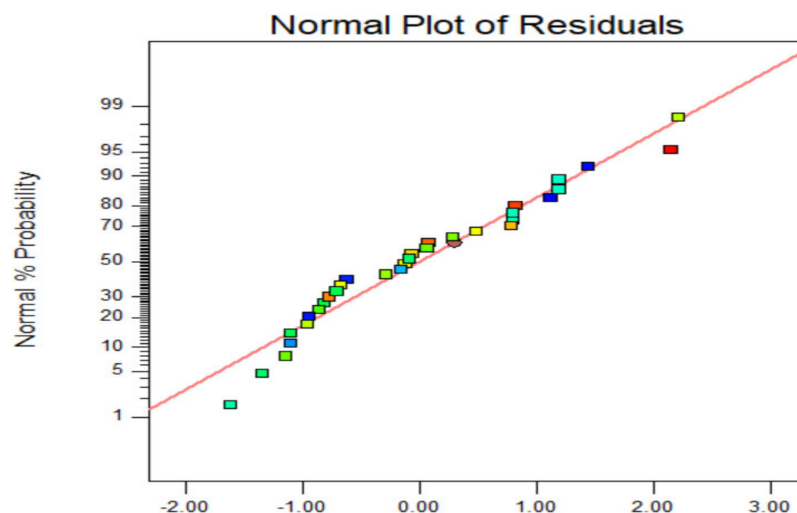


Figure 3. The plot of internally studentized residuals vs. predicted.

The least-squares residuals are an essential tool for evaluating the model's adequacy and accuracy [38]. Figure 4 shows the plot of residuals vs. the predicted response. The model's residual plots are distributed evenly above and below the horizontal axis and proved their quality [39]. Thus, the results indicated good maximum response predictions and constant variance and adequacy of the quadratic models.

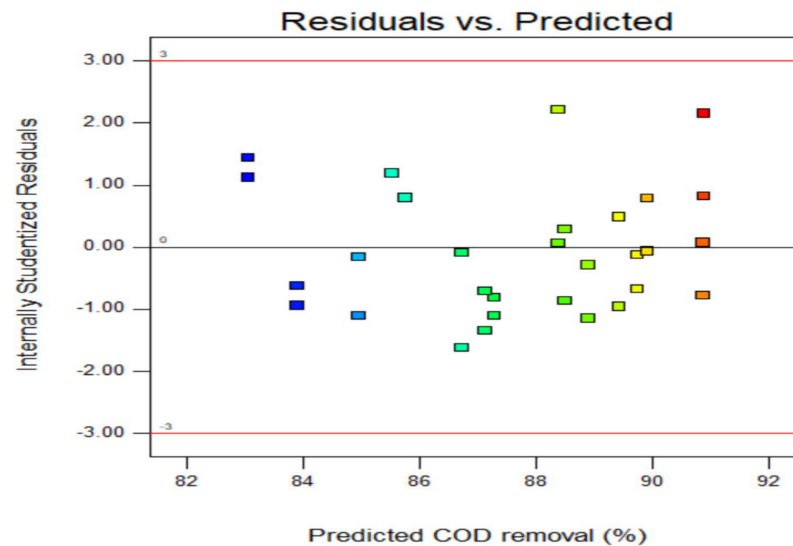


Figure 4. The plot of internally studentized residuals vs. predicted response.

3.3. Analysis of Response

To visualise and assess the independent variables' influence, the three-dimensional (3D) response surface plots and their corresponding two-dimensional (2D) contour maps for the modelled response were constructed. The 3D plot is handy in evaluating the system's behaviour within the experimental design [40]. These plots endorsed the previously presented ANOVA study by identifying the relative contributions to the operating parameters' response. The different single and interacting effects of parameters A, B, and C on COD removal are displayed.

As shown in Figure 5a,b, the plot illustrates an elliptical shape, while Figure 6a,b and Figure 7a,b are circular. According to Sathian et al. (2014) [41], the curve's elliptical shape suggests a strong interaction between the two variables, and a circular shape indicates no interaction between the variables. Therefore, the contour's oval form in Figure 5a reflects the reciprocal interactions of temperature and NaCl concentration.

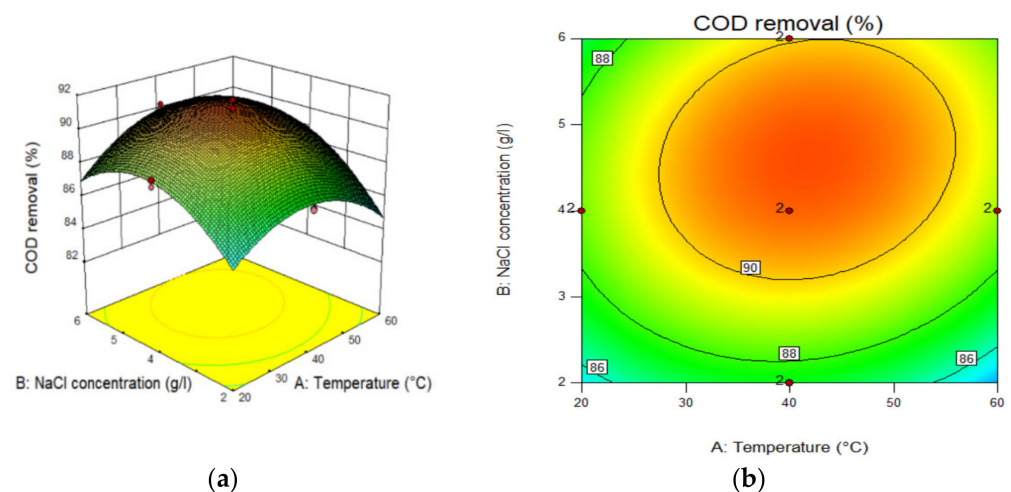


Figure 5. (a) Three-dimensional (3D) response graph and (b) contour plot for the effect temperature and NaCl concentration.

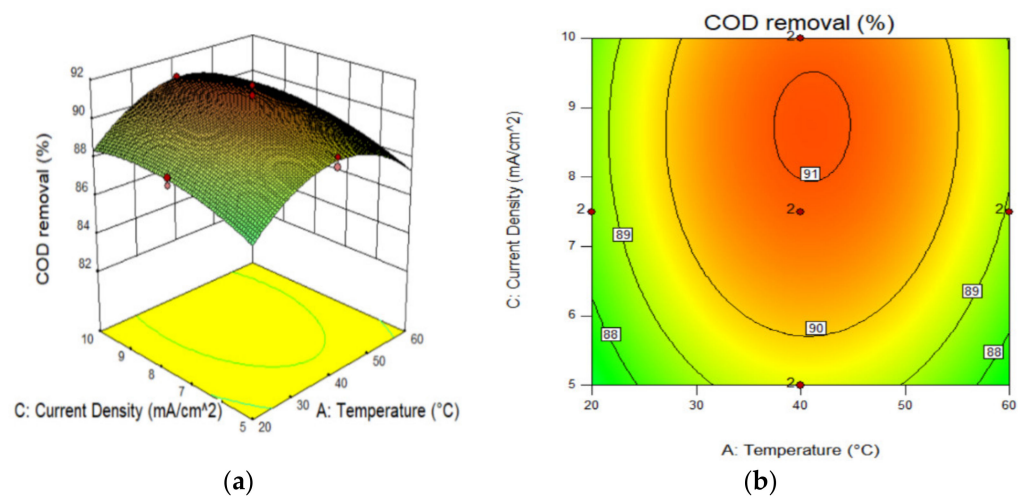


Figure 6. (a) Three-dimensional (3D) response graph and (b) contour plot for the effect of temperature and current density.

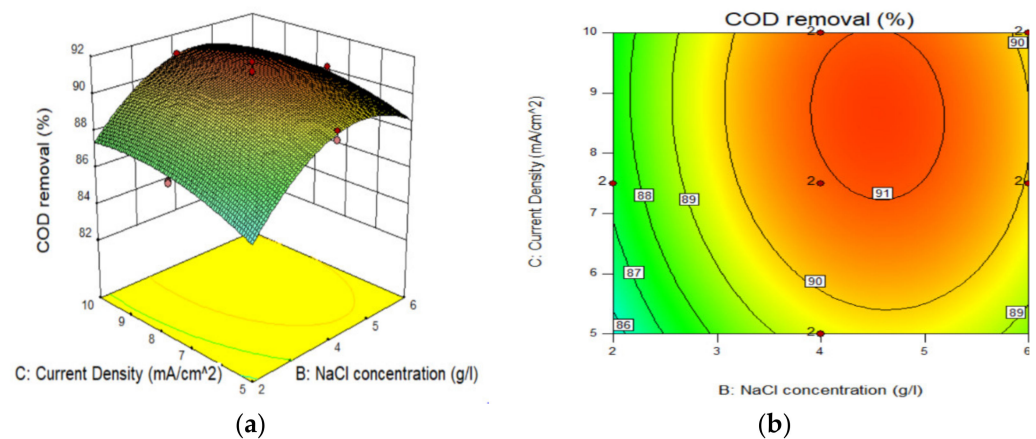


Figure 7. (a) Three-dimensional (3D) response graph and (b) contour plot for the NaCl concentration and current density.

As shown in Figure 5a,b, the effects of temperature and NaCl concentration were determined when the current density was at its centre point (7.5 mA/cm²). When the temperature and NaCl concentration were at a low level (20 °C and 5 mA/cm²), COD removal was low. Therefore, a significant improvement in COD removal can be obtained by increasing the temperature and NaCl concentration to 42 °C and 4.5 g/L, respectively.

The interaction between temperature and current density and NaCl concentration & current density was statistically insignificant, as shown in Figure 6a,b and Figure 7a,b, respectively.

This section showed that current density had little interaction with both temperature and NaCl concentration. However, temperature and NaCl concentration were shown to have strong interactions. This information obtained and the mathematical models developed will be used to evaluate for scale-up.

3.4. Economic Evaluation

The EO process's technical feasibility is usually evaluated in terms of COD removal efficiency, while the energy consumption evaluates the economic feasibility. The energy consumption was calculated using Equation (3) [17].

$$\text{Energy Consumption} = \frac{UIt}{V(COD_0 - COD_t)} \quad (3)$$

where U is the applied voltage; I is the applied current (Amp); V is the volume of treated wastewater (L); t is operating time (h), COD_0 is the initial COD of wastewater (mg/L), and COD_t is the treated COD of wastewater at electrolysis time.

The energy consumption for EO treatment was calculated as 0.214 kWh/ kg COD for optimum COD removal at a current density, temperature and electrolyte (NaCl) concentration were 7.5 mA/cm², 42 °C and 4.5 g/L, respectively. Comparable results were obtained in good agreement with the data reported in the literature [16,42]. Titanium was selected because of its practicality, stability, and cost-effective material for electrochemical oxidation of organic pollutants [16,43].

The EO process exhibited lower energy consumption than other treatment technologies such as ozonation and Fenton oxidation [44]; photocatalysis [45] due to the pollutants' complete mineralisation under optimal conditions. Therefore, the EO treatment process can be economically feasible for PRW applications' treatment from an energy consumption perspective due to the COD removal efficiency. Along with its capability of treating high-strength wastewater, the EO process provides a significant advantage of the technology to be adopted by a wide range of different wastewater treatment applications [46–49]. Experimental discoveries showed that electrochemical oxidation with Ti/IrO₂–Ta₂O₅ electrodes could be an alternative as a treatment technique for PRW wastewater effluent.

RSM assists with understanding the behaviour of a system and guidance to evaluate the significances of different situations. The mathematical optimisation part in design expert allows maximising the desirability application [34]. This optimisation process was carried out to maximise the COD reduction efficiency of PRW.

4. Conclusions

Process optimisation of the EO process of COD removal for PRW treatment was studied using BBD with RSM. The temperature, current density, and electrolyte concentration applied were investigated as the primary operating parameters on COD removal efficiency. At an optimised temperature of 42 °C, applied current density of 7.5 mA/cm², and a mid-NaCl concentration of 4.5 g/L, the EO process with dimensional stable anodes (DSAs) could efficiently remove 99.83% COD in 12 hours. The BBD data demonstrated significant effects of the variables studied and their interactive effects in reducing COD. Furthermore, the ANOVA results showed that the COD removal efficiency model was significant and adequate, as proven by the statistical indexes, including lack of fit, coefficient of variation, and proper precision. Therefore, RSM could be effectively adopted to optimise the operating multivariable in complex EO processes.

Author Contributions: Conceptualisation, S.C. and M.A.; methodology, S.C. and M.A.; formal analysis, S.C.; investigation, S.C.; resources, M.A.; data curation, S.C.; writing—original draft preparation, S.C.; writing—review and editing, M.A.; supervision, M.A., project administration, M.A. All authors have read and agreed to the published version of the manuscript.

Funding: This research received no external funding.

Institutional Review Board Statement: Not applicable.

Informed Consent Statement: Not applicable.

Data Availability Statement: The data presented in this study are available on request from the corresponding author. The data are not publicly available due to internal policies.

Acknowledgments: The authors are thankful to the Department of Chemical Engineering and the Environmental Engineering Research Group (EnvERG) for their support. The Research Directorate of Cape Peninsula University of Technology (CPUT), South Africa, for the postgraduate student assistance and their commitment towards the article processing charges (APC), as well as the African Union Mwalimu Nyerere for the student scholarship.

Conflicts of Interest: The authors declare no conflict of interest.

Abbreviations

ANOVA: analysis of variation; BBD: Box-Behnken design; COD: chemical oxygen demand; DC: direct current; DSA: dimensional stable anode; EC: electron conductivity; EO: electrochemical oxidation; NaCl: sodium chloride; OFAT: one factor at a time; PRW: petroleum refinery wastewater; RSM: response surface methodology; R^2 : coefficient of determination; T: temperature.

References

1. Coelho, A.; Castro, A.V.; Dezotti, M.; Sant'Anna, G.L.J. Treatment of petroleum refinery sourwater by advanced oxidation processes. *J. Hazard. Mater.* **2006**, *137*, 178–184. [[CrossRef](#)] [[PubMed](#)]
2. Diya'uddeen, H.B.; Daud, W.M.A.W.; Aziz, A.R.A. Treatment technologies for petroleum refinery effluents: A review. *Process Saf. Environ. Prot.* **2010**, *89*, 95–105. [[CrossRef](#)]
3. Ratshomo, K.; Nembahe, R. *2018 South African Energy Sector Report*; Department of Energy: Pretoria, South Africa, 2018; ISBN 9781920435141.
4. Bwapwa, J.K. Review on Main Issues Causing Deterioration of Water Quality and Water Scarcity: Case Study of South Africa. *Environ. Manag. Sustain. Dev.* **2018**, *7*, 14. [[CrossRef](#)]
5. Gasim, H.A.; Kutty, S.R.M.; Isa, M.H.; Isa, M.P.M. Treatment of Petroleum Refinery Wastewater by using UASB Reactors. *Int. J. Chem. Biol. Eng.* **2012**, *6*, 174–177.
6. Guo, S.; Li, G.; Qu, J.; Liu, X. Improvement of acidification on dewaterability of oily sludge from flotation. *Chem. Eng. J.* **2011**, *168*, 746–751. [[CrossRef](#)]
7. Myburgh, D.P.; Aziz, M.; Roman, F.; Jardim, J.; Chakawa, S. Removal of COD from Industrial Biodiesel Wastewater Using an Integrated Process: Electrochemical-Oxidation with IrO₂-Ta₂O₅/Ti Anodes and Chitosan Powder as an Adsorbent. *Environ. Process.* **2019**, *6*, 819–840. [[CrossRef](#)]
8. Gao, J.; Yan, J.; Liu, Y.; Zhang, J.; Guo, Z. A novel electro-catalytic degradation method of phenol wastewater with Ti/IrO₂-Ta₂O₅ anodes in high-gravity fields. *Water Sci. Technol.* **2017**, *76*, 662–670. [[CrossRef](#)] [[PubMed](#)]
9. Park, H.; Bak, A.; Ahn, Y.Y.; Choi, J.; Hoffmann, M.R. Photoelectrochemical performance of multi-layered BiO x-TiO 2/Ti electrodes for degradation of phenol and production of molecular hydrogen in water. *J. Hazard. Mater.* **2012**, *211*, 47–54. [[CrossRef](#)]
10. Shestakova, M.; Bonete, P.; Gómez, R.; Sillanpää, M.; Tang, W.Z. Novel Ti/Ta₂O₅-SnO₂ electrodes for water electrolysis and electro-catalytic oxidation of organics. *Electrochim. Acta* **2014**, *120*, 302–307. [[CrossRef](#)]
11. Mukimin, A.; Vistanty, H.; Zen, N. Oxidation of textile wastewater using cylinder Ti/β-PbO₂ electrode in electro-catalytic tube reactor. *Chem. Eng. J.* **2015**, *259*, 430–437. [[CrossRef](#)]
12. Ani, I.J.; Akpan, U.G.; Olutoye, M.A.; Hameed, B.H. Photocatalytic degradation of pollutants in petroleum refinery wastewater by TiO₂-and ZnO-based photocatalysts: Recent development. *J. Clean. Prod.* **2018**, *205*, 930–954. [[CrossRef](#)]
13. Sillanpää, M.; Shestakova, M. *Electrochemical Water Treatment Methods-Fundamentals, Methods and Full Scale Application*; Butterworth-Heinemann: Oxford, UK, 2017; ISBN 9780128114629.
14. Feng, Y.; Yang, L.; Liu, J.; Logan, B.E. Electrochemical technologies for wastewater treatment and resource reclamation. *Environ. Sci. Water Res. Technol.* **2016**, *2*, 800–831. [[CrossRef](#)]
15. Arslan, G.; Yazici, B.; Erbil, M. The effect of pH, temperature and concentration on electrooxidation of phenol. *J. Hazard. Mater.* **2003**, *124*, 37–43. [[CrossRef](#)]
16. Yao, J.; Mei, Y.; Xia, G.; Lu, Y.; Xu, D.; Sun, N.; Wang, J.; Chen, J. Process optimisation of electrochemical oxidation of ammonia to nitrogen for actual dyeing wastewater treatment. *Int. J. Environ. Res. Public Health* **2019**, *16*, 2931. [[CrossRef](#)] [[PubMed](#)]
17. Raju, G.B.; Karuppiyah, M.T.; Latha, S.S.; Parvathy, S.; Prabhakar, S. Treatment of wastewater from synthetic textile industry by electrocoagulation-electrooxidation. *Chem. Eng. J.* **2008**, *144*, 51–58. [[CrossRef](#)]
18. Delgarm, N.; Sajadi, B.; Azarbad, K.; Delgarm, S. Sensitivity analysis of building energy performance: A simulation-based approach using OFAT and variance-based sensitivity analysis methods. *J. Build. Eng.* **2018**, *15*, 181–193. [[CrossRef](#)]
19. Ahmed, S.A.; Abdella, M.A.A.; El-Sherbiny, G.M.; Ibrahim, A.M.; El-Shamy, A.R.; Atalla, S.M.M. Application of one-factor-at-a-time and statistical designs to enhance α-amylase production by a newly isolate Bacillus subtilis strain-MK1. *Biocatal. Agric. Biotechnol.* **2019**, *22*, 101397. [[CrossRef](#)]
20. Frey, D.D.; Sudarsanam, N. An adaptive one-factor-at-a-time method for robust parameter design: Comparison with crossed arrays via case studies. *J. Mech. Des. Trans. Asme* **2008**, *130*, 1–18. [[CrossRef](#)]
21. Swati; Ghosh, P.; Thakur, I.S. Biodegradation of pyrene by Pseudomonas sp. ISTPY2 isolated from landfill soil: Process optimisation using Box-Behnken design model. *Bioresour. Technol. Rep.* **2019**, *8*, 100329. [[CrossRef](#)]
22. Bas, D.; Boyaci, I.H. Modeling and optimisation I: Usability of response surface methodology. *J. Food Eng.* **2007**, *78*, 836–845. [[CrossRef](#)]
23. Nor, N.M.; Mohamed, M.S.; Loh, T.C.; Foo, H.L.; Rahim, R.A.; Tan, J.S.; Mohamad, R. Comparative analyses on medium optimisation using one-factor-at-a-time, response surface methodology, and artificial neural network for lysine-methionine biosynthesis by Pediococcus pentosaceus RF-1. *Biotechnol. Biotechnol. Equip.* **2017**, *31*, 935–947. [[CrossRef](#)]
24. Anderson, M.J.; Whitcomb, P.J. *RSM Simplified: Optimising Processes Using Response Surface Methods for Design of Experiments*, 2nd ed.; Productivity Press: New York, NY, USA, 2016.

25. Fukuda, I.M.; Pinto, C.F.F.; Moreira, C.D.S.; Saviano, A.M.; Lourenço, F.R. Design of experiments (DoE) applied to pharmaceutical and analytical quality by design (QbD). *Braz. J. Pharm. Sci.* **2018**, *54*, 1–16. [[CrossRef](#)]
26. Ahmadi, M.; Ghanbari, F. Optimizing COD removal from greywater by photoelectro-persulfate process using Box-Behnken design: Assessment of effluent quality and electrical energy consumption. *Environ. Sci. Pollut. Res.* **2016**, *23*, 19350–19361. [[CrossRef](#)]
27. Ten Chan, Y.; Tan, M.C.; Chin, N.L. Application of Box-Behnken design in optimisation of ultrasound effect on apple pectin as sugar replacer. *LWT Food Sci. Technol.* **2019**, *115*, 108449. [[CrossRef](#)]
28. Gulen, B.; Demircivi, P. Adsorption properties of fluoroquinolone type antibiotic ciprofloxacin into 2:1 dioctahedral clay structure: Box-Behnken experimental design. *J. Mol. Struct.* **2020**, 1206. [[CrossRef](#)]
29. Scialdone, O.; Randazzo, S.; Galia, A.; Silvestri, G. Electrochemical oxidation of organics in water: Role of operative parameters in the absence and in the presence of NaCl. *Water Res.* **2009**, *43*, 2260–2272. [[CrossRef](#)] [[PubMed](#)]
30. Sharma, S.; Aygun, A.; Simsek, H. Electrochemical treatment of sunflower oil refinery wastewater and optimisation of the parameters using response surface methodology. *Chemosphere* **2020**, *249*, 126511. [[CrossRef](#)]
31. Samarghandi, M.R.; Nemattollahi, D.; Asgari, G.; Shokoohi, R.; Ansari, A.; Dargahi, A. Electrochemical process for 2,4-D herbicide removal from aqueous solutions using stainless steel 316 and graphite Anodes: Optimisation using response surface methodology. *Sep. Sci. Technol. Phila.* **2019**, *54*, 478–493. [[CrossRef](#)]
32. Aziz, M.; Ojumu, T. Exclusion of estrogenic and androgenic steroid hormones from municipal membrane bioreactor wastewater using UF/NF/RO membranes for water reuse application. *Membranes* **2020**, *10*, 37. [[CrossRef](#)] [[PubMed](#)]
33. Abbas, Z.N.; Abbar, A.H. Application of response surface methodology for optimisation of phenol removal from a simulated wastewater using rotating tubular packed bed electrochemical reactor. *Egypt. J. Chem.* **2020**, *63*, 3925–3936.
34. Mukwevho, M.J.; Maharajh, D.; Chirwa, E.M.N. Evaluating the effect of pH, temperature, and hydraulic retention time on biological sulphate reduction using response surface methodology. *Water* **2020**, *12*, 2662. [[CrossRef](#)]
35. Tian, S.; Hao, C.; Xu, G.; Yang, J.; Sun, R. Optimization conditions for extracting polysaccharide from *Angelica sinensis* and its antioxidant activities. *J. Food Drug Anal.* **2017**, *25*, 766–775. [[CrossRef](#)] [[PubMed](#)]
36. Thangam, R.; Suresh, V.; Kannan, S. Optimised extraction of polysaccharides from *Cymbopogon citratus* and its biological activities. *Int. J. Biol. Macromol.* **2014**, *65*, 415–423. [[CrossRef](#)]
37. Darvishmotevalli, M.; Zarei, A.; Moradnia, M.; Noorisepehr, M.; Mohammadi, H. Optimization of saline wastewater treatment using electrochemical oxidation process: Prediction by RSM method. *MethodsX* **2019**, *6*, 1101–1113. [[CrossRef](#)]
38. Zhang, Y.J.; Li, Q.; Zhang, Y.X.; Wang, D.; Xing, J.M. Optimization of Succinic acid fermentation with *Actinobacillus succinogenes* by response surface methodology (RSM). *J. Zhejiang Univ. Sci. B* **2012**, *13*, 103–110. [[CrossRef](#)]
39. Sales Solano, A.M.; Costa de Araújo, C.K.; Vieira de Melo, J.; Peralta-Hernandez, J.M.; Ribeiro da Silva, D.; Martínez-Huitle, C.A. Decontamination of real textile industrial effluent by strong oxidant species electrogenerated on diamond electrode: Viability and disadvantages of this electrochemical technology. *Appl. Catal. B Environ.* **2013**, *130–131*, 112–120. [[CrossRef](#)]
40. Esfandyari, Y.; Mahdavi, Y.; Seyedsalehi, M.; Hoseini, M.; Safari, G.H.; Ghanbari, G.M.; Kamani, H.; Jaafari, J. Degradation and biodegradability improvement of the olive mill wastewater by peroxi-electrocoagulation/electrooxidation- electroflotation process with bipolar aluminum electrodes. *Environ. Sci. Pollut. Res.* **2015**, *22*, 6288–6297. [[CrossRef](#)]
41. Sathian, S.; Rajasimman, M.; Radha, G.; Shanmugapriya, V.; Karthikeyan, C. Performance of SBR for the treatment of textile dye wastewater: Optimisation and kinetic studies. *Alex. Eng. J.* **2014**, *53*, 417–426. [[CrossRef](#)]
42. Körbahti, B.K.; Turan, K.M. Evaluation of Energy Consumption in Electrochemical Oxidation of Acid Violet 7 Textile Dye using Pt/Ir Electrodes. *J. Turk. Chem. Soc. Sect. A Chem.* **2016**, *3*, 75. [[CrossRef](#)]
43. Martínez-Huitle, C.A.; Panizza, M. Electrochemical oxidation of organic pollutants for wastewater treatment. *Curr. Opin. Electrochem.* **2018**, *11*, 62–71. [[CrossRef](#)]
44. Cañizares, P.; Paz, R.; Sáez, C.; Rodrigo, M.A. Costs of the electrochemical oxidation of wastewaters: A comparison with ozonation and Fenton oxidation processes. *J. Environ. Manag.* **2009**, *90*, 410–420. [[CrossRef](#)] [[PubMed](#)]
45. Escudero, C.J.; Iglesias, O.; Dominguez, S.; Rivero, M.J.; Ortiz, I. Performance of electrochemical oxidation and photocatalysis in terms of kinetics and energy consumption. New insights into the p-cresol degradation. *J. Environ. Manag.* **2017**, *195*, 117–124. [[CrossRef](#)] [[PubMed](#)]
46. Woisetschläger, D.; Humpl, B.; Koncar, M.; Siebenhofer, M. Electrochemical oxidation of wastewater-Opportunities and drawbacks. *Water Sci. Technol.* **2013**, *68*, 1173–1179. [[CrossRef](#)] [[PubMed](#)]
47. Zöllig, H.; Remmele, A.; Morgenroth, E.; Udert, K.M. Removal rates and energy demand of the electrochemical oxidation of ammonia and organic substances in real stored urine. *Environ. Sci. Water Res. Technol.* **2017**, *3*, 480–491. [[CrossRef](#)]
48. Ukundimana, Z.; Omwene, P.I.; Gengec, E.; Can, O.T.; Kobya, M. Electrooxidation as post treatment of ultrafiltration effluent in a landfill leachate MBR treatment plant: Effects of BDD, Pt and DSA anode types. *Electrochim. Acta* **2018**, *286*, 252–263. [[CrossRef](#)]
49. Iskurt, C.; Keyikoglu, R.; Kobya, M.; Khataee, A. Treatment of coking wastewater by aeration assisted electrochemical oxidation process at controlled and uncontrolled initial pH conditions. *Sep. Purif. Technol.* **2020**, *248*, 117043. [[CrossRef](#)]